SAR image segmentation using B-Spline deformable contours

María J. Gambini*, Julio C. Jacobo*,
Marta E. Mejail* and Alejandro C. Frery**

*Universidad de Buenos Aires, FCEyN,
Departamento de Computación, Buenos Aires,
Argentine Republic, {jgambini, jacobo, marta}@dc.uba.ar
**Universidade Federal de Pernambuco, CiN,
Recife-PE, Brasil, frery@cin.ufpe.br

Abstract

Synthetic Aperture Radar (SAR) images are corrupted by a signal-dependent non-additive noise called speckle. Many statistical models have been proposed to describe this noise, aiming at the development of specialized techniques for image improvement and analysis. One of the most important parameters in SAR imagery is texture or roughness that, within some statistical models, can be characterized by a scalar. This quantity is obscured by speckle noise. The $\mathcal{G}$ distribution is a quite flexible model that succeeds in describing areas with a wide range of roughness, from pastures (homogeneous) to urban areas (extremely heterogeneous). This distribution exhibits a remarkably good performance within urban areas, while other distributions considered in the literature for SAR data, namely Gamma and $\mathcal{K}$, fail to fit that type of data. In addition to its expressiveness, a sub-case of the $\mathcal{G}$ distribution, the $\mathcal{G}^0$ distribution is mathematically more tractable than the classical $\mathcal{K}$ law. These parameters will be estimated in order find the transition points between regions with different degrees of homogeneity. In order to determine the boundaries of urban areas in SAR imagery B-Splines is here proposed. After the specification of an initial region within the city to be segmented, the algorithm determines the positions of the B-Spline control points maximizing an objective function. The proposed algorithm is tested on synthetic SAR images in order to measure its performance.

Keywords: SAR, B-Splines, Active Contours, $\mathcal{G}$ distribution

1 Introduction

Region boundary finding is an important issue in remote sensing image analysis and many techniques have been studied to solve this problem. In the particular case of region boundary determination in SAR images, the use of Active Statistic Contours for data following the Gamma probability law, has been developed by O. Germain *et al.* [3].

The technique proposed in this work is based on B-Spline boundary fitting and was originally developed A. Blake *et al.* [1], the main difference being that it has been adapted to SAR images, using the $\mathcal{G}$ distribution as a general data model.

The $\mathcal{G}$ distribution, proposed by A. Frery *et al.* [2], fits SAR data more satisfactorily than the traditional distributions, specially in the case of heterogeneous areas like cities or forests, for which the Γ and the $\mathcal{K}$ distribution exhibit a suboptimal performance. From the $\mathcal{G}$ distribution, several sub-cases can be derived. One of them, the $\mathcal{G}^0$ distribution, is interesting because it fits SAR data as well as the $\mathcal{G}$ distribution does, and is mathematically and computationally more tractable. This particular model is the one that will be used in this work.

The boundary finding process we describe here, begins with the determination of zones of interest. Each of them includes one region for which we are going to extract the corresponding boundary. These zones of interest are given by B-Spline curves, determined by their control points. Then, a series of segments normal to each B-Spline is drawn on the image, and the image data lying on them are extracted. For each normal segment, the transition point, that is, the point belongs to the region's boundary, is determined. This determination is based on the estimated values for the statistical parameters of the data. Then, for each region, the contour sought is given by the B-spline curve that fits these transition points.

The structure of this paper is as follows: section 2 describes the statistical model used here for SAR data, section 3 gives an introduction to B-Spline curve fitting , section 4 specifies the criterium used to determine the transition points and explains the region fitting algorithm, and finally, section 5 shows the obtained results.

2 The $\mathcal{G}$ distribution for SAR data

SAR images can be modelled as the product of two independent random fields, one corresponding to the backscatter X and other to the *speckle* noise Y. In this manner,

$$Z = X \cdot Y \tag{1}$$

models the return Z under the multiplicative model as the result of the product of the random field Y that models the *speckle* noise, inherent to every coherent imaging system, and the random field X that models backscatter's variability.

For amplitude data, the speckle noise Y is modelled as a $\Gamma^{1/2}(n, n)$ distributed random variable, where n is the number of looks used to generate the SAR image. This parameter is constant for the whole image.
For this type of data too, the backscatter X is considered to obey a Generalized Inverse Gaussian law, denoted as $\mathcal{N}^{-1/2}(\alpha, \lambda, \gamma)$, (see A. Frery *et al.* [2]).

For particular values of the parameters of the $\mathcal{N}^{-1/2}$ distribution, the $\Gamma^{1/2}(\alpha, \lambda)$, and the $\Gamma^{-1/2}(\alpha, \gamma)$ distributions are obtained. These, in turn, give rise to the $\mathcal{K}$ and the $\mathcal{G}^0$ distributions for the return Z, respectively.

Given the mathematical tractability and descriptive power of the $\mathcal{G}^0$ distribution, it represents an atractive choice for SAR data modelling.

The density function for this model is given by

$$f_{\mathcal{G}^0}(z) = \frac{2n^n \Gamma(n-\alpha)}{\gamma^\alpha \Gamma(-\alpha)\Gamma(n)} \frac{z^{2n-1}}{(\gamma + z^2 n)^{n-\alpha}}, \qquad -\alpha, \gamma, z > 0,\ n \geq 1, \tag{2}$$

The moments of the $\mathcal{G}^0$ distribution are:

$$E_{\mathcal{G}^0}(Z^r) = \left(\frac{\gamma}{2n}\right)^{r/2} \frac{\Gamma(-\alpha + r/2)}{\Gamma(-\alpha)} \frac{\Gamma(n + r/2)}{\Gamma(n)}, \qquad -\alpha > r, \tag{3}$$

In this work the $\mathcal{G}^0$distribution will be used to estimate the statistical parameters . In this work the $\mathcal{G}^0$distribution will be used as the SAR data model. These data are characterized by their distribution parameters and are analyzed through the estimation of these parameters [4].

2.1 Estimation

As presented in equation (2) the parameter α of the $\mathcal{G}_A^0$ distribution is defined for negative values. Estimation is crucial in many applications and, besides that, the value of this parameter is immediately interpretable in terms of target's roughness when the $\mathcal{G}_A^0$ model is used; this interpretability will be treated in detail in section 2.2.

Several parameter estimation techniques are available, being the most remarkable ones those based on maximum likelihood, on sample moments or substitution method (MO for short), on order statistics and on data transformations.

In this work MO estimation is used. This technique is based on replacing theoretical moments by sample observations, and then calculating the unknown parameters.

To estimate the α and γ parameters it is necessary then to estimate two moments. In this work moments of order 1/2 and 1, namely $m_{1/2}$ and m_1 respectively, will be used. These moments are, through equation (3), given by

$$m_{1/2} = \left(\frac{\gamma}{n}\right)^{1/4} \frac{\Gamma(-\alpha - 1/4)\Gamma(n + 1/4)}{\Gamma(-\alpha)\Gamma(n)}, \alpha < -1/4 \tag{4}$$

$$m_1 = \left(\frac{\gamma}{n}\right)^{1/2} \frac{\Gamma(-\alpha - 1/2)\Gamma(n + 1/2)}{\Gamma(-\alpha)\Gamma(n)}, \alpha < -1/2. \tag{5}$$

Then, using (4) and (5), $\widehat{\alpha}$ can be determined as the solution of the following equation:

$$g(\widehat{\alpha}) - \zeta = 0, \tag{6}$$

where

$$g(\widehat{\alpha}) = \frac{\Gamma^2\left(-\widehat{\alpha} - \frac{1}{4}\right)}{\Gamma(-\widehat{\alpha})\Gamma\left(-\widehat{\alpha} - \frac{1}{2}\right)} \tag{7}$$

and

$$\zeta = \frac{\widehat{m}_{1/2}^2}{\widehat{m}_1} \frac{\Gamma(n)\Gamma(n+\frac{1}{2})}{\Gamma^2(n+\frac{1}{4})}, \tag{8}$$

and then substituting the value of $\widehat{\alpha}$ in equation (4) or in equation (5) to find $\widehat{\gamma}$.

It can be noticed that $g(\widehat{\alpha})$ converges asymptotically to one. As ζ is a random variable that can take values greater than one, there are cases for which equation (6) does not have a solution. The lower the value of the α parameter, the higher probability that a solution for equation (6) does not exist.

2.2 Parameter interpretation

One of the most important features of the $\mathcal{G}_A^0$ distribution is that the estimated values of the parameter α have immediate interpretation in terms of roughness. For values of α near zero, the imaged area presents very heterogeneous gray values, as is the case of urban areas. As we move to less heterogeneous areas like forests, the value of α diminishes, reaching its lowest values for homogeneous areas like pastures and certain types of crops. This is the reason why this parameter is regarded to as a roughness or texture measure. Fig. 1 depicts this interpretation, with the levels of roughness associated to light shades; the values shown are inspired in those presented by A. Frery *et al.* [2], where real data are used. This interpretability is a consequence of the use of the multiplicative model, and it is in complete accordance with the parameter α of the $\mathcal{K}$ distributions, see C. Oliver *et al.* [7].

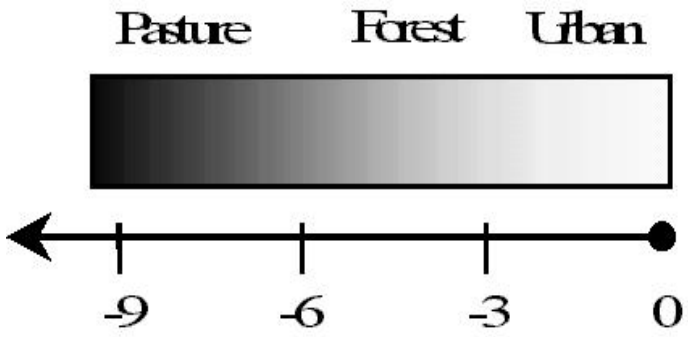

Figure 1: Graphical representation of the interpretation of the roughness parameter.

The parameter γ of the $\mathcal{G}_A^0$ distribution is a scale parameter, that is, let W be a $\mathcal{G}_A^0(\alpha, \gamma, n)$ distributed random variable, then

$$\frac{1}{\sqrt{\gamma}} W \sim \mathcal{G}_A^0(\alpha, 1, n) \tag{9}$$

In this manner, this parameter is related to the amplitude of the backscatter. Our sight is more sensitive to variations in mean value than to those related to roughness and, therefore, it is easy to find situations were areas with different roughness parameters are perceived as alike, whilst areas with different scale parameters are immediately discriminated regardless of their roughness.

The mode of density function for $\mathcal{G}_A^0$ distributed random variables depends on the roughness parameter α. As can be seen in Fig. 2 and in Fig. 3, the more homogeneous the area, the closer the mode is to zero [5].

3 B-spline Representation

For the sake of clarity, we now present a brief theoretical review of B-spline representation of contours. For more details, see A. Blake *et al.* [1] and D. Rogers *et al.* [8].

Let $\{Q_0, ..., Q_{N_B-1}\}$ be a set of control points, where

$$Q_i = (x_i, y_i)^t, \tag{10}$$

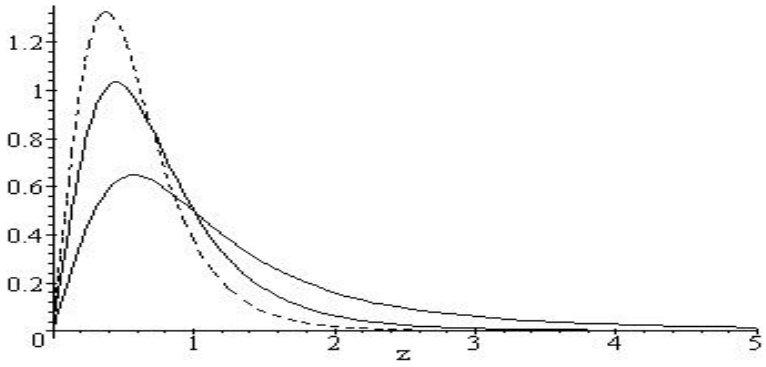

Figure 2: Three $\mathcal{G}_A^0(\alpha, 1, 1)$ densities with $\alpha = -1$ (solid), $\alpha = -2$ (dash) and $\alpha = -3$ (dot resp.).

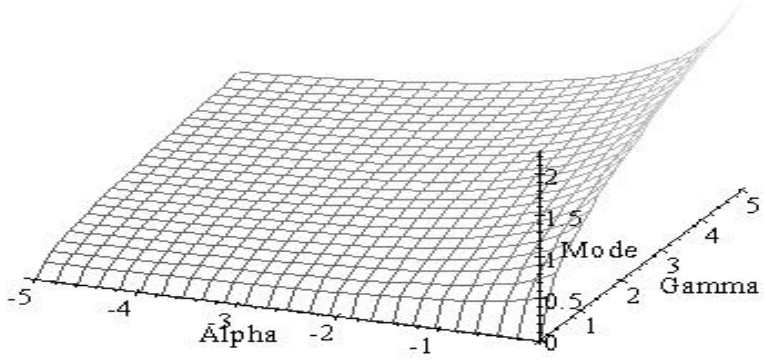

Figure 3: The mode of a $\mathcal{G}_A^0(\alpha, \gamma, 1)$ ditribution.

a B-spline curve is defined as a weighted sum of N_B basis functions $\mathrm{B}_{n,d}(s)$, with $0 \leq s \leq L$, and $0 \leq n \leq N_B - 1$. Let $\{s_0 < s_1 < s_2 < ... < s_{L-1}\} \subset R$ be the set of knots. By definition, the B-spline curve is a polynomial function of degree $d-1$, within each interval $[s_i, s_{i+1}]$. The constructed spline function is $r(s)$:

$$r(s) = (x(s), y(s))^t . \tag{11}$$

being

$$r(s) = \sum_{n=0}^{N_B-1} \mathrm{B}_{n,d}(s)\, Q_n, \tag{12}$$

and being

$$x(s) = \mathrm{B}^t(s).Q^x \tag{13}$$
$$y(s) = \mathrm{B}^t(s).Q^y \tag{14}$$

where the basis functions vector $\mathrm{B}(s)$, of N_B components, is given by

$$\mathrm{B}(s) = (\mathrm{B}_{0,d}(s), ..., \mathrm{B}_{N_B-1,d}(s))^t , \tag{15}$$

and the weight vectors are

$$Q^x = (x_0, x_1, ..., x_{N_B-1})^t , \tag{16}$$

and

$$Q^y = (y_0, y_1, ..., y_{N_B-1})^t . \tag{17}$$

This can be expressed compactly in matrix notation:

$$r(s) = B(s).Q = I_2 \otimes \mathrm{B}^t(s) \begin{pmatrix} Q^x \\ Q^y \end{pmatrix}, \tag{18}$$

where $B(s)$ is a $2 \times 2N_B$ real matrix given by

$$B(s) = \begin{pmatrix} \mathrm{B}^t(s) & 0 \\ 0 & \mathrm{B}^t(s) \end{pmatrix}, \tag{19}$$

The symbol $\otimes$ denotes the Kroneker product of two matrices, and I_2 is the 2×2 identity matrix.

In this work we use closed curves with $d = 3$ or $d = 4$. To describe this type of curves, we use the periodic B-spline basis functions.

3.1 B-spline curve fit

The problem of determining a polygon that generates a B-spline curve with known number of control points, N_B was developed by D. Rogers *et al.* [8]. We now present a brief review of this subject.

A set of data points in the image plane is given by

$$\{D_0, D_1, ..., D_{k-1}\}, \tag{20}$$

where

$$D_i = (x_i, y_i)^t, \qquad i = 0, ..., k-1, \tag{21}$$

and the spline that best-fits them is sought. Then the components D_i must satisfy

$$x_i = \mathrm{B}^t(t_i) Q^x, \tag{22}$$

$$y_i = \mathrm{B}^t(t_i) Q^y, \tag{23}$$

for certain values of t_i, where $i = 0, ...k$, and $N_B \leq k$.

This linear system is more compactly written in matrix form as

$$D = K \begin{pmatrix} Q^x & Q^y \end{pmatrix}, \tag{24}$$

where $k \times N_B$ real matrix K is given by

$$K_{ij} = B_{i,d}(t_j), \qquad i = 0, ..., k,\ j = 0, ..., N_B - 1, \tag{25}$$

and

$$D = (D_0, D_1, ..., D_k)^t. \tag{26}$$

In the more general case, $N_B < k$, K could be not a square matrix. In that case we would have to use the pseudo-inverse matrix form:

$$\begin{pmatrix} Q^x & Q^y \end{pmatrix} = \left(K^t K\right)^{-1} K^t D. \tag{27}$$

One useful approximation for the parameter value $\{t_0, ...t_{k-1}\}$ is

$$t_0 = 0, \tag{28}$$

$$t_l = \frac{\sum_{i=1}^{l} \|D_i - D_{i-1}\|}{\sum_{i=1}^{k-1} \|D_i - D_{i-1}\|} \quad , \ l \geq 1. \tag{29}$$

The knot set to build the B-spline basis functions, is chosen arbitrarily.

3.2 Norm for B-spline curves

The curve norm is important for comparing the performance between two curve fits. Since B-spline curves are represented as weight vectors $\begin{pmatrix} Q^x & Q^y \end{pmatrix}^t$, we define the norm of a curve in terms of these vectors as

$$\|r\| = \left\| \begin{pmatrix} Q^x & Q^y \end{pmatrix}^t \right\|_{\mathcal{U}},$$

where

$$\left\| \begin{pmatrix} Q^x & Q^y \end{pmatrix}^t \right\|_{\mathcal{U}} = \begin{pmatrix} Q^x & Q^y \end{pmatrix} \mathcal{U} \begin{pmatrix} Q^x & Q^y \end{pmatrix}^t,$$

and

$$\mathcal{U} = \frac{1}{L}\int_0^L U(s)U^t(s)\,ds.$$

Now we can define a distance between two curves r_1 and r_2 as

$$d\left(r_1, r_2\right) = \left\|r_1 - r_2\right\|. \tag{30}$$

4 Boundary Detection

We assume that the scene is constituted by a set of regions and a background. Each of these regions and the background are considered to be random fields of independent, identically $\mathcal{G}^0$ distributed random variables, characterized by the values of their statistical parameters α and γ.
In order to find a curve that fits a particular region's boundary, a search zone around that region is established. This zone of interest is specified by means of a B-Spline, which in turn is determined by several control points. Then, a series of segments normal to the B-Spline, is drawn on the image.
For the ith normal segment $n^{(i)}$ to a generic region, given by

$$n^{(i)} = \left(z_1^{(i)}, \ldots, z_m^{(i)}\right), \tag{31}$$

we consider the following partition

$$Z_k^{(i)} \sim \mathcal{G}^0\left(\alpha_r, \gamma_r\right), \quad k = 1, \ldots, j \tag{32}$$

$$Z_k^{(i)} \sim \mathcal{G}^0\left(\alpha_b, \gamma_b\right), \quad k = j+1, \ldots, m, \tag{33}$$

where, for each value of the index k , the $z_k^{(i)}$ is a realization of the $Z_k^{(i)}$ random variable, α_r and γ_r are the parameters that characterize the region, and α_b and γ_b are the parameters that characterize the background. Then, for each normal segment, the likelihood function will be the objective function to be maximized, and is given by:

$$l = \prod_{k=0}^{j} \Pr(z_k; \alpha_r, \gamma_r). \prod_{k=j+1}^{m} \Pr(z_k; \alpha_b, \gamma_b) \tag{34}$$

In order to find the transition points we actually maximize the log-likelihood function $L = \ln l$, given by

$$L = \sum_{k=0}^{j} \ln(f_{\mathcal{G}^0}\left(z_k; \alpha_r, \gamma_r\right)) + \sum_{k=j+1}^{m} \ln(f_{\mathcal{G}^0}\left(z_k; \alpha_b, \gamma_b\right)). \tag{35}$$

Then, according to formula (2)

$$\begin{aligned} L &= \sum_{k=0}^{j} \ln\left(\frac{2n^n\Gamma\left(n-\alpha_r\right)z_k^{2n-1}}{\gamma_r^{\alpha_r}\Gamma\left(-\alpha_r\right)\Gamma\left(n\right)\left(\gamma_r + nz_k^2\right)^{n-\alpha_r}}\right) + \\ &\quad + \sum_{k=j+1}^{m} \ln\left(\frac{2n^n\Gamma\left(n-\alpha_b\right)z_k^{2n-1}}{\gamma_b^{\alpha_b}\Gamma\left(-\alpha_b\right)\Gamma\left(n\right)\left(\gamma_b + nz_k^2\right)^{n-\alpha_b}}\right). \end{aligned}$$

Finally, the index value that corresponds to the transition point j^* is calculated as

$$j^* = \arg\max_j L. \tag{36}$$

The sketch of the procedure is as follows:

1. A region of interest is determined by means of a B-Spline, which in turn is determined by several control points
2. A series of segments, which are normal to the B-Spline, is drawn on the image
3. For each segment, the relevant statistical parameters of SAR data are estimated and a border point for each normal segment is detected.
4. With these points, a new B-Spline curve is built, which lies on the region boundary.

5 Results and Conclusions

A synthetic image, under the $\mathcal{G}^0$ model, with three different city-like areas with $\alpha = -1.5, -2.1, -2.7$ and a background with $\alpha = -10.0$ was generated. All of the parameters are considered unknown and they are estimated from the image. Initial boundaries (thin lines) and final boundaries (thick lines) can be seen on Fig. 4. On this figure, three types of initialization were used: accross region boundaries (upper left), inside region (upper right) and outside region (lower middle).

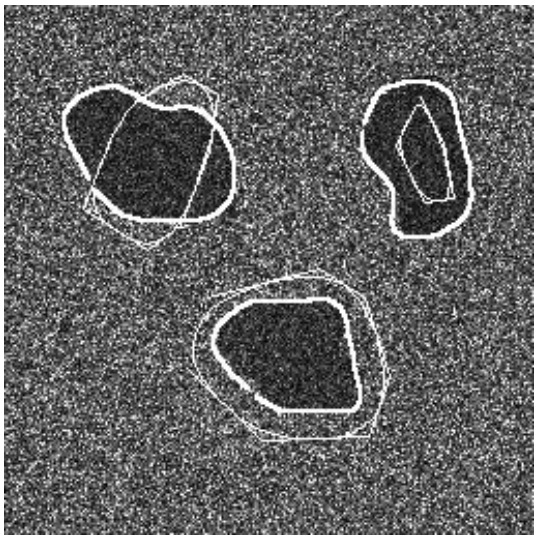

Figure 4: Synthetic image, under the $\mathcal{G}^0$ model, with three different regions with $\alpha = -1.5, -2.1, -2.7$ and a background with $\alpha = -10.0$ with initial and final boundaries indicated.

The synthetic image on Fig. 5 shows an urban area generated with $\alpha = -3.0$ inside a B-Spline curve and a background area generated with $\alpha = -10.0$. The fitted curve was generated using the algorithm explained above, see subsection 3.2). The distance between real and the estimated curves was calculated using the definition given in formula 30. The result of the curve fit is visually good, in accordance with the value of 0.14 obtained for the distance between both curves.

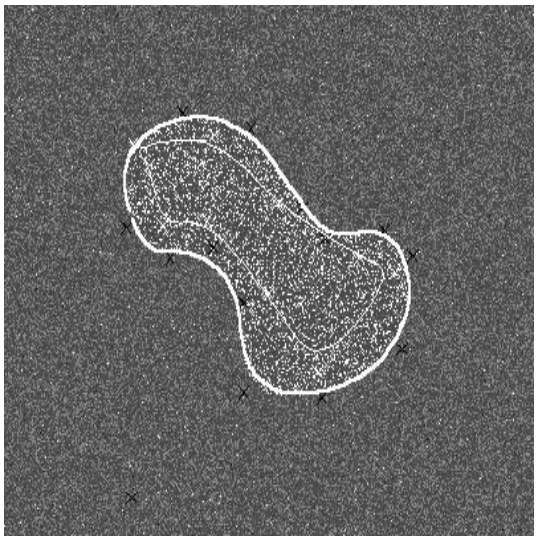

Figure 5: Curve fit evaluation: distance between real and estimated region boundary equal to 0.14.

On Fig. 6, the values of a typical objective function, taken along one of the line segments that were laid normal to one of the initial region boundaries, can be observed. The position of the maximum is considered to correspond to the transition point between both regions, according to formula (36)

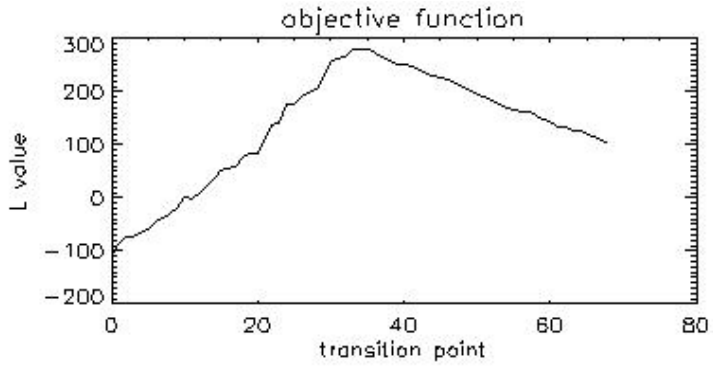

Figure 6: Typical values of the objective function for all the possible positions for the transition point between two regions.

In this paper, a new approach to urban area segmentation in SAR images using B-spline deformable contours, is described. The example shown here, using a synthetic image, the boundaries of several urban regions were found analyzing only the zones of interest, which lowers the computational cost and improves the method's performance.

References

[1] A. Blake and M. Isard "Active Contours". Springer Verlag, 1998.

[2] A. C. Frery, H.J. Muller, C. C. F. Yanasse and S. J. S. Sant'Anna: "A model for extremely heterogeneous clutter" IEEE Trans. Geosc. Rem. Sens., Vol. 35, 1997, pp. 648-659

[3] O.,Germain and P. Réfrégier "Edge detection and localization in SAR images: a comparative study of global filtering and active contour approaches.

[4] M. Mejail, A. Frery, J. Jacobo and O. Bustos: "Approximation of Distributions for SAR Images: Proposal, Evaluation and Practical Consequences" Latin American Applied Research. Vol. 13, 2000, pp. 37-49.

[5] M. Mejail, J. Jacobo and A. Frery: "Statiscal Classification of SAR Images Using a General and Tractable Multiplicative Model" International Journal of Remote Sensing, 2002, in press.

[6] H.J. Muller, A. C. Frery, J. Jacobo-Berlles, M. Mejail and J. R. Moreira: "The harmonic branch of themultiplicative model: properties and applications". EUSAR2000, pp. 603-606

[7] C. Oliver and S. Quegan: "Understanding Synthetic Aperture Radar Images" Boston: Artech House, 1998.

[8] D. Rogers and J. A. Adams: "Mathematical Elements for Computer Graphics" McGraw-Hill, 2nd edition, 1990.